

# Geometry of Black Holes and Multi-Black-Holes in 2+1 dimensions<sup>1</sup>

Dieter R. Brill

University of Maryland, College Park, MD 20742, USA

## Contents

- I. Introduction
- II. (2+1)-Dimensional Initial Values in Stereographic Projection
  - A. The single, non-rotating black hole
  - B. Non-rotating multi-black-holes
  - C. “Black Hole” Universe Initial Values
- III. Time Development: Enter the Raychaudhuri Equation
- IV. Time Development in Stereographic Projection
  - A. The BTZ black hole spacetime
  - B. Multi-Black-Hole Spacetimes
- V. Black Holes with Angular Momentum
- VI. Analogous 3+1-Dimensional Black Holes
- VII. Conclusions

## I. Introduction

On this special occasion I bring greetings to Prof. Raychaudhuri from the Relativity Group at the University of Maryland, a university that had the good fortune to have Prof. Raychaudhuri as a visitor about the time that “his” equation was first explored and began to shed light on so many interesting and important issues in General Relativity. I myself missed much of this history because I did not arrive at Maryland until the 1970’s, so I am particularly grateful not to miss the celebration today, and I am indeed honored to participate in this happy occasion.

My topic is not directly concerned with the Raychaudhuri equation, but it is of course not hard to establish the connection with his elegant ideas; what would be hard is to give a talk in modern General Relativity in which the Raychaudhuri equation would not enter in some fashion, so pervasive is its influence in our field.

It is perhaps surprising that gravity in 2-dimensional space, even as a “toy model,” should be of any interest, because a local analysis of vacuum Einstein gravity in 2+1 dimensions reveals little contents. Namely, Einstein’s equations specify the Ricci tensor, which in 2+1 dimensions specifies the Riemann tensor, which in turn gives a complete local description of gravity: spacetime is flat, or has constant curvature  $\Lambda$  if there is a cosmological constant. In particular, there is no “Newtonian limit” of 2+1 dimensional gravity. It was therefore surprising when, about three years ago, 2+1 dimensional black hole solutions were discovered. Their nature is due to the *global* structure of spacetime, there is no local gravitational interaction associated with them.

---

<sup>1</sup>Lecture given at “Raychaudhuri session,” ICGC-95 conference, Pune (India), December 1995

In 3+1 dimensions, exact solutions containing more than one black hole are known only in special cases. The difficulty is that an exact multi-black-hole solution would have to describe in one metric all the physics associated with such configurations, including their motion in orbits about each other, the gravitational radiation emitted, the consequent energy loss of the black hole system, and its possible eventual collapse and merger into a single asymptotically stationary black hole. No such complicated behavior is expected in 2+1 dimensions, for example because there is no gravitational radiation. Hence it is reasonable to expect exact multi-black-hole solutions in this case.

I will show how to construct such solutions, and explore the geometry of the spacetimes so obtained. The results are interesting not least for the fascinating way in which the 2+1 dimensional spacetime succeeds in imitating most of those properties expected of 3+1 dimensional multi-black-holes that can be achieved by the global structure. One may therefore hope that these solutions can serve as simplified models for exploring the more difficult questions of black hole physics, for example those connected with quantization; but I will not attempt to show such applications here.

## II. (2+1)-Dimensional Initial Values in Stereographic Projection.

All 2+1 spacetimes with a given negative cosmological constant are locally isometric, as we have seen. One important global difference between such spacetimes is the topology. More complicated topologies can be obtained from simpler ones through identifications by certain isometries. The topologically simplest of these is anti-de Sitter space; it is the universal cover of all others.

In the usual quotient space construction that implements the identification process the isometries have no fixed points and are spacelike. This is so because one wants to avoid singularities or closed timelike lines in the quotient space. In the case of black holes, singularities are familiar and accepted if they are hidden behind horizons. To understand such geometrical relationships it is convenient to use a representation of anti-de Sitter space that is the extension, to spacetimes of constant negative curvature, of the description due to Poincaré for the 2-dimensional Riemannian case. These representations are conformal and can be considered a stereographic projection of the curved space into the plane or into flat three-space.

We begin with the embedding of anti-de Sitter (adS) space in a flat space of one higher dimension. This is analogous to the standard embedding of the round sphere in Euclidean space, but for negative curvature the embedding space must have indefinite metric, of a signature with one more negative direction than that of the adS space itself. For 2+1 dimensional adS space, we need a four-dimensional flat space of signature  $(- - ++)$  and metric

$$ds^2 = -dT^2 - dU^2 + dX^2 + dY^2 \tag{1}$$

The hyperbolic surface

$$-T^2 - U^2 + X^2 + Y^2 = -\ell^2. \tag{2}$$

then represents a solution of the vacuum Einstein equations with negative cosmological constant  $\Lambda = -1/\ell^2$ . (This embedded spacetime is periodic in the time direction; true adS spacetime is the universal cover of this periodic spacetime, obtained by “unwinding” about the XY axis. Our stereographic maps will always project less than one period, so that this distinction will not make any difference.)

The stereographic map of a 2-sphere embedded in the standard way in Euclidean 3-space can be obtained by projection from the “North” pole on a plane tangent at the “South pole.” For the hyperboloidal surface of Eq (2), the analog of the North pole can be taken to be the point  $(0, \ell, 0, 0)$ , and the analog of the tangent space to the South pole is the “plane”  $U = -\ell$ . A point  $X^\mu$  ( $\mu = 0, \dots, 3$  with  $U = X^1$ ) in the hyperboloidal surface projects to a point with coordinates

$$x^\mu = \frac{2\ell X^\mu}{U + \ell} \quad X^\mu \neq U \quad (3a)$$

in three-dimensional Minkowski space. The surface metric in these coordinates is

$$ds^2 = \left( \frac{1}{1 - r^2} \right)^2 (-dt^2 + dx^2 + dy^2) \quad \text{where} \quad r^2 = \frac{-t^2 + x^2 + y^2}{4\ell^2}, \quad (3b)$$

clearly a *conformal* map.

To picture the projection in no more than three dimensions we consider subspaces, such as the “initial” spacelike surface  $T = 0 = t$ ,  $U > 0$ . This surface has zero extrinsic curvature (it is “totally geodesic”). Because adS space has constant negative curvature, the intrinsic geometry of this surface must likewise have constant negative curvature — it is hyperbolic 2-space,  $H^2$ . Its embedding in (1+2) Minkowski space is obtained by setting  $T = 0$ ,  $U > 0$  in Eqs (1) and (2). This embedding and its stereographic projection on the plane  $U = -\ell$  is shown in Fig. 1. (The embedded surface is one of the two spacelike hyperboloids of constant spacetime distance  $\ell$  from the origin.)

The Figure shows that in the stereographic projection all points of the hyperboloid lie within a “limit circle” of finite radius  $2\ell$ . This representation of the two-dimensional space of constant negative curvature is known as the *Poincaré disk*, whose properties are very well understood. The stereographic projection translates any figure or theorem of the “hyperbolic geometry” in the space  $H^2$  of constant negative curvature to a figure or theorem of Euclidean geometry. Thus the figures drawn in the Poincaré disk are not merely cartoons, but show geometrical relationships as faithfully as figures of Euclidean geometry.

The metric of the Poincaré disk is given by Eq (3b) with  $t = 0$ . From it we can deduce the shape of *geodesics* in the disk. Alternatively we can characterize geodesics on the hyperboloid as intersections with planes through the origin. In either approach we find the standard result: geodesics are represented in the disk as arcs of circles that intersect the limit circle at right angles (as judged by the flat, Euclidean geometry of the plane). Two such geodesics either intersect inside the limit circle, or touch on the limit circle, or intersect nowhere. In the latter two cases they are called parallel and ultraparallel, respectively.

The hyperboloid is invariant under (isochronous) Lorentz transformations, therefore the symmetry group of  $H^2$  is  $SL(2, R) \sim SU(1, 1)$ . The boosts have no fixed points on the hyperboloids; the corresponding transformations on the Poincaré disk are called *transvections*.<sup>2</sup> Because any point on the hyperboloid can be boosted to the special point  $U = \ell$ ,  $X = Y = 0 = T$ , any point on the disk can be transvected to the origin. It is often useful to make such a transvection, without loss of generality, to get a simple representation of some geometrical feature. We can

---

<sup>2</sup>Isometries of  $H^2$  can be classified into elliptic (one fixed point, we call these rotations), parabolic (a fixed point at infinity), and hyperbolic (the transvections).

think of the Poincaré disk as a magnifying glass that gives an undistorted and largest image only at its center, and this magnifying glass can be centered on any point to see a true image of its immediate neighborhood. For example, rotations appear as Euclidean rotations of the plane if the center of rotation is placed at the origin; and geodesics through the origin are Euclidean straight lines.

### A. The single, non-rotating black hole

The (2+1)-dimensional black holes of Bañados, Teitelboim and Zanelli [1] with zero angular momentum are described by the metric

$$ds^2 = -\left(-M + (r/\ell)^2\right) dt^2 + \frac{dr^2}{-M + (r/\ell)^2} + r^2 d\phi^2. \quad (4)$$

That this is locally equivalent to the surface of Eq (2) is shown by the embedding

$$\begin{aligned} X &= \sqrt{-\ell^2 + \frac{r^2}{M}} \cosh \frac{\sqrt{M}}{\ell} t & Y &= \frac{r}{\sqrt{M}} \sinh \sqrt{M} \phi \\ T &= \sqrt{-\ell^2 + \frac{r^2}{M}} \sinh \frac{\sqrt{M}}{\ell} t & U &= \frac{r}{\sqrt{M}} \cosh \sqrt{M} \phi, \end{aligned} \quad (5)$$

which transforms the metric (1) into the metric (4). Note that the spacelike surface  $t = 0$  corresponds to the embedding with  $T = 0$  shown in Fig. 1. The coordinate lines described by Eq (4) on this embedded surface project on the Poincaré disk to the lines shown in Fig. 2.

What distinguishes the BTZ metric globally is the identification  $\phi \equiv \phi + 2\pi$ . In the embedding of the surface  $t = 0 = T$  a change in  $\phi$  corresponds to a Lorentz boost that leaves the  $X$ -axis fixed, hence it is a transvection in the corresponding Poincaré disk. The radial lines  $\phi = \text{const}$  clearly are geodesics, hence fit smoothly together. Thus the isometry that leads to the initial state of a BTZ black hole is a transvection connecting two ultraparallels, such as the two shown as thick curves in Fig. 2. The limit circle is thereby divided into two parts, which represent the two asymptotically adS regions of the BTZ black hole. The “throat” (horizon) of the black hole is the minimal, “vertical” geodesic between the two thick curves.

### B. Non-rotating Multi-Black-Holes

Instead of identifying the two geodesics in one Poincaré disk as in Fig. 2, we can use two identical copies of Fig. 2 and identify geodesics that correspond when the two copies are superimposed (Fig. 3). To obtain a BTZ black hole of the same mass by this “doubling,” the range of  $\phi$  in each disk should be half that in the single disk construction.

By a similar construction [2] we can obtain a space with more than two asymptotically adS regions, describing several black holes.<sup>3</sup> We start with a region between several mutually ultraparallel geodesics. We shall call this region the “original region.” We make two copies and identify corresponding geodesics. Figure 4 shows this doubling procedure for the case of three

---

<sup>3</sup>Strictly speaking, the construction gives us initial values. That these do develop into spacetimes with horizons and black holes will be shown in Section IV. For now we can think of the horizons as apparent horizons.

geodesics. Each of the three regions between pairs of geodesics near the limit circle is isometric to the asymptotic region of a single BTZ black hole of suitable mass  $M$ . To specify the mass parameter we recall that any pair of ultraparallels have a unique (minimal) geodesic segment that is normal to both. For a single BTZ black hole this segment corresponds to the horizon, and its length is  $\pi\ell\sqrt{M}$ . (This is half the horizon length because the black hole geometry is obtained from the original region by doubling.) For the multi-black-hole geometry the isometry of an asymptotic region to a BTZ black hole can be extended at least to the minimal segment, so it is reasonable to associate with each asymptotic region a mass (as measured from that region) given by the same formula, using the minimal segment between corresponding adjacent ultraparallels of the original region. We shall call these minimal segments the horizon of the corresponding black hole. In general, there will be as many separate, asymptotically adS regions, and hence as many black holes, each with its own mass parameter, as there are geodesics bounding the original region.

The identifications of the Figure can also be described by a group of isometries, so that the identified space is the quotient of  $H^2$  by this group. To find these isometries we first note that any transvection in the Poincaré disk can be completely described by a geodesic segment. (Namely, the segment specifies the plane through the origin of Fig. 1 in which its pre-image lies; the segment's endpoints specify the boost parameter of the Lorentz transformation that leaves the plane invariant; and the image of the Lorentz transformation is the desired transvection.) The group of isometries is generated by the transvections specified by twice the normal segments of the original region that describe the horizons. (The factor two comes about because we are doubling the original region. For  $n$  horizons only  $n - 1$  of the isometries are independent, Eq (6).)

In the original region, the horizons and the parts of the ultraparallels between them form a polygon with  $2n$  sides and with all interior angles being right angles (Fig. 5a). The length of the horizon  $h_i$  measures the mass of the  $i^{\text{th}}$  black hole; the segment  $s_i$  between horizons  $h_{i-1}$  and  $h_{i+1}$  is the shortest distance between these horizons, and can be identified with the “distance” between the two corresponding black holes. In such a polygon of  $2n$  sides, when  $2n - 3$  consecutive sides are given, then the remaining three sides are determined. In other words, we can specify  $n - 1$  black holes and the distances between adjacent ones, and are then forced to have an  $n^{\text{th}}$  black hole at definite distance from the first and the  $n - 1^{\text{st}}$  one. To express this relation algebraically we think of the Lorentz transformation  $L_i$  in the embedding picture, specified by the  $i^{\text{th}}$  side. Because the polygon closes, the product of the  $2n$  transformations must be unity,

$$\prod_i^{2n} L_i = \mathbb{1}, \quad (6)$$

a set of three conditions. For example, two horizons of mass  $m_1$  and  $m_2$  at a distance  $d$  require a third horizon of mass  $M$  such that [3]

$$\cosh(\pi\sqrt{M}) = \cosh(d/\ell) \sinh(\pi\sqrt{m_1}) \sinh(\pi\sqrt{m_2}) - \cosh(\pi\sqrt{m_1}) \cosh(\pi\sqrt{m_2}) \geq 1 \quad (7)$$

We see that not all choices of  $m_1$ ,  $m_2$  and  $d$  are possible, because the r.h.s. must not be less than unity. For given  $m_1$ ,  $m_2$  this places a lower limit on  $d$ . As  $d$  approaches the lower limit,  $M$  tends to zero and its distance from the other black holes tends to infinity. The hexagon degenerates into a pentagon with an ideal vertex at infinity (Fig. 5b). (If  $d$  is less than the lower

limit, the pentagon has a finite vertex with an angle less than a right angle. The doubling would then lead to a conical singularity at this vertex, corresponding to a “particle” analogous to a cosmic string in 3+1 dimensions. Such particles are not considered here; see however [3], [4]).

To obtain a valid polygon for our construction, the inequality of Eq (7) must not be violated by any pair of masses. We can therefore think of the three-particle configuration as the basic building block of the higher ones: we cut off an asymptotic region at its horizon and “thread” it to another such configuration, similar to the way a plumber can thread together several tees to obtain a connected manifold with a larger number of openings (Fig. 6). Note that there is additional arbitrariness in the “twist” angle between adjacent “tees,” which makes these multi-black-holes more general than those obtained by doubling of a polygon.

### C. “Black Hole” Universe Initial Values

The horizons of any multi-black-hole configuration are closed geodesics, so they have vanishing extrinsic curvature. If the intrinsic geometry (the length, hence the mass parameter) of two horizons is the same, then they can be identified. For example, the horizons in Fig. 6b can be identified pairwise as shown by the dotted arrows. There are then no more asymptotic regions, we have a closed universe containing several “wormholes”.<sup>4</sup> The Gauss-Bonnet theorem implies that the Euler characteristic of such a configuration must be negative, hence the universe constructed according to Fig. 6 has the minimum number (two) of wormholes. At each identification there is an arbitrary angle of twist, so this type of universe is characterized by three mass and three twist parameters, with the masses at each tee having to satisfy the inequality (7).

Instead of eliminating all asymptotic regions we could keep one or several, for example by making only one of the two dotted-arrow identifications in Fig. 6, yielding black hole configurations with internal topological structure.<sup>5</sup>

### III. Time Development: Enter the Raychaudhuri Equation

The Multi-Black-Hole initial values we discussed in the last section differ from adS initial values only in the global structure; in particular, they are locally homogeneous and isotropic. Therefore the time development is completely described by that of the volume element,  $\sqrt{g}$ . It is the *Raychaudhuri Equation* that gives us this time development.

In the context of an analysis of development in proper time  $\tau$  a convenient form of the (2+1)D Raychaudhuri equation is

$$\dot{K} + K^{ij}K_{ij} + 2(p - \Lambda) = 0.$$

The local isotropy demands isotropic time development,  $K_{ij} = \frac{1}{2}K g_{ij}$ , with  $K = \frac{1}{\sqrt{g}} \frac{\partial \sqrt{g}}{\partial \tau}$ . In the absence of matter we have  $p = 0$ , hence

$$\dot{K} + \frac{1}{2}K^2 - 2\Lambda = 0$$

---

<sup>4</sup>These are not black holes in the usual sense because once the asymptotic region is eliminated, there is no longer a horizon around them. They do, however, have the classic wormhole topology, and the geometry at each wormhole there is an apparent horizon, with the geometry in its vicinity being the same as that near the (true) horizon of a BTZ black hole.

<sup>5</sup>The interesting case when there is only one asymptotic region and internal structure will be the subject of a separate publication [6].

The solution that satisfies the initial condition  $K = 0$  is

$$K = -\left(\frac{2}{\ell}\right) \tan\left(\frac{\tau}{\ell}\right)$$

Thus after a time  $\tau = \pi\ell/2$ ,  $K$  diverges. This is the first consequence usually obtained from the Raychaudhuri equation: there is a conjugate point where the normal geodesics to the initial surface intersect. Because of the homogeneity of our model, all these geodesics intersect in one point ( $r = 0 = t$  in BTZ coordinates), whether they start inside the horizon or outside.

The identification that is used to construct the initial state must of course extend to these geodesics. It yields a nonsingular space if the corresponding isometries are transitive, that is, if there is no fixed point. This is of course no longer true at the point where the geodesics intersect. In Riemannian spaces a fixed point leads to a conical singularity; in Lorentzian spaces a fixed point in whose neighborhood the isometry is a boost leads to a “non-Hausdorff” singularity [5]. It is customary to regard such singularities as analogous to the black hole curvature singularity of higher dimensions, and define a horizon that hides this singularity in an analogous way.

The Raychaudhuri analysis specifies, in this isotropic case, the entire time development in Raychaudhuri time<sup>6</sup> of any Multi-Black-Hole solution as it follows from time symmetric initial data. Namely, the conformal representation of constant- $\tau$  surfaces is the same as the initial surface  $\tau = 0$ , as for example in Fig. 4a; only the conformal factor decreases, reaching zero at  $\tau = \pi\ell/2$ . But note that a BTZ  $r$ -coordinate, as in Fig. 2a, measures the circumference of circles at all times, hence if all space sections are represented by one constant diagram in the Poincaré disk, then any  $r$ -coordinate lines should move outward as  $\tau$  increases, to compensate for the decrease in the conformal factor. The geodesics of test particle with zero initial velocity are represented by a point at rest in the diagram, their inward fall being exhibited by the outward motion of the  $r = \text{const}$  curves.

This representation shows only the initial data’s domain of dependence and not its analytic continuation beyond the Cauchy horizon. For example, the outward-moving  $r = \text{const}$  lines (which have finite acceleration), as well as geodesics with initial velocity, and light rays accumulate at the limit circle in a finite time. (It is amusing that their subsequent development can be described as motion outside the limit circle, in a metric with a changed signature.) The Raychaudhuri time slicing therefore represents accurately only the interior part of a multi-black-hole solution. For the closed universes of Section IIC, which have no asymptotic region, it does represent the nonsingular part of the time development in its entirety. The exterior of any horizon is of course the same as that of a BTZ black hole of the same mass parameter. To understand how the exterior and interiors fit together, so that horizons can be analyzed, we return to the stereographic projection.

#### IV. Time Development in Stereographic Projection

To understand the stereographic, conformal map (3b) away from the surface  $T = 0$ , consider first the section  $Y = 0$  (Figure 7). In this case the projection fills the space between two limit *hyperbolas*. This is the spacetime analog of the Poincaré disk. We call it the *Minkowski disk*. We can again think of it as a magnifying glass that distorts except at the center — away from the center the magnification decreases to zero in spacelike directions, and increases to infinity

---

<sup>6</sup>I use this convenient term for the time-orthogonal slicing of spacetime with proper time ( $\tau$ ) coordinate that corresponds to constant lapse function  $N = |\partial/\partial\tau|$ .

in timelike directions. Unlike the projection of the constant curvature spaces of positive definite metric, this is not a map of the complete spacetime, but only of the past (resp. future) of the “point at infinity.” One can verify that the geometrical properties of the Poincaré disk still hold if circles are everywhere replaced by hyperbolas. For example, spacelike geodesics are hyperbolas that meet the limit hyperbolas normally in the Minkowski sense (or not at all).

In Figure 7 the initial “surface”  $T = 0$  that extends to infinity is projected by conformal distortion to a finite-length diameter of the limit hyperbola. The  $r = 0$  singularities of a BTZ black hole occur  $90^\circ$  away from the initial surface, in the plane  $U = 0$ . One of these is shown in the Figure as a dotted hyperbola. The projection of that hyperbola on the plane is also a hyperbola (not shown), asymptotic to the dotted lightlike lines. Thus the stereoscopic projection of that section is very similar to the Kruskal diagram of a Schwarzschild black hole, except that null infinity  $\mathcal{I}$  is represented at a finite distance — it is the limit hyperbola.

If we rotate the hyperboloid with initial “surface” and singular hyperbola by  $90^\circ$  (but leave the projection center and the plane fixed), we thereby center our lens on the singularity, which in the projection is now represented by the finite-length diameter of the limit hyperbola. The initial surface is now the dotted hyperbola. Because it lies in a plane parallel to the projection plane, the conformal factor is constant, so that its projection involves no distortion.

#### A. The BTZ black hole spacetime

We are now ready to consider the projection in three dimensions. The 2+1 adS space is now represented by the interior of a limit hyperboloid. We call this interior the Minkowski ball. The horizontal section through the center of this figure is a disk — it is the Poincaré disk that we discussed as the  $T = 0$  initial state. To construct black holes we now merely have to extend the identifications introduced in Section II consistently throughout the Minkowski ball.

Figure 8a shows the Minkowski ball, the Poincaré disk embedded as an initial surface, a geodesic through the center of the Poincaré disk, and the Minkowski disk normal to the Poincaré disk at this geodesic. We can move the geodesic and its Minkowski disk to another (ultraparallel) position by means of an isometry (a kind of transvection of the Minkowski ball, which however has fixed points – as we shall see). The result is shown in Figure 8b. Not surprisingly the totally geodesic Minkowski disk now becomes a hyperboloid. The two ultraparallels on the Poincaré disk (of Figs. 8a and b, respectively) are suitable for identification to form the initial state of a BTZ black hole, as we have seen in Section II. The identification can be extended to the corresponding Minkowski disks, since their intrinsic geometry is the same and their extrinsic curvature vanishes. The resulting spacetime, that is adS space modulo the isometry, is the unique development of the initial data – it is a BTZ black hole spacetime.

The Minkowski disks of Figure 8 intersect in a spacelike hyperbola. Its points are fixed points of the isometry, and represent the non-Hausdorff singularity at  $r = 0$  of the BTZ spacetime. Figure 9 is a combination of Figs. 8a and b, cut up and separated along a vertical plane. Some BTZ coordinate lines are plotted in this vertical plane, showing again their similarity to the Kruskal coordinates of Schwarzschild spacetime. The BTZ spacetime is the heavily-outlined part of the right half of the figure; its front and back surfaces correspond to  $\phi = 0$  and  $2\pi$ , respectively, and are to be identified.

So far our stereographic projection has been centered on the initial surface. It is also interesting to center it on the singularity. The figure is then a three-dimensional version of the

projection discussed in connection with Figure 7, with the dotted hyperbola being the initial surface. As before, the singularity is then a line, and it is still true that on the initial surface, the conformal factor is constant, so the initial surface can be shown without distortion, as a hyperboloid in Minkowski space (Fig. 10). Furthermore, the plane Minkowski disks ( $\phi_{BTZ} = \text{const}$ ) are represented as planes intersecting the singular line. Since that line, and hence the planes, pass through the origin, the planes intersect the initial surface in (ultraparallel) geodesics, as they should in order to generate a BTZ black hole after identification. Null infinity  $\mathcal{I}$  now ends at a finite point, so it is easy to draw the associated horizon — it is just the backward Minkowski lightcone from that point.

## B. Multi-Black-Hole Spacetimes

The above spacetime construction can be extended to the multi-black-hole case. Mathematically, the isometries of the initial surface that define the multi-black-hole initial values extend to all of adS space, so the multi-black-hole spacetime is the quotient of adS space by the isometries so extended. In the stereographic projection we would have to add further hyperboloids to Figs. 8 and 9, and double in the way described in Section II the spacetime between them. Pairs of hyperboloids intersect in spacelike hyperbolas, and all of the hyperboloids intersect in one common point, where any geodesic motion with initially vanishing velocity ends — this was one of the lessons learned from the Raychaudhuri equation. Thus the non-Hausdorff singularity is represented by several hyperbolas radiating out from the common point. Geodesics that start out with nonzero velocity end on one of the hyperbolas, depending into which black hole they fall. Null geodesics either end similarly or go to a  $\mathcal{I}$  in an asymptotic region. The two possible behaviors allow the usual definition of horizons as the boundary of the region that is in the past of  $\mathcal{I}$ .

The identification surfaces are simplest in the stereographic projection that is centered on the common point of the singularity, because they are then planes as in Fig. 10. These planes form a pyramid with spacelike edges, and the physical region is the intersection of the inside of the pyramid with the Minkowski ball (Fig. 11). The ends of each  $\mathcal{I}$  occur where one of the edges pierces the limit hyperboloid. The backward lightcones from these ends form the horizon, as will be discussed in a separate paper [6].

Here we will explore only the section of a four-black-hole horizon in a plane of symmetry  $S$ . We return to the Kruskal-like representation of a projection centered on the initial surface and show the relevant features in Figure 12. The plane of symmetry cuts through two of the horizons on the initial surface, labeled  $h_1$  and  $h_3$ . The spacetime diagram shows the entire history in  $S$  of these horizons. Unlike the single BTZ black hole horizons, these horizons have a past endpoint on the singularity associated with the *other* black hole. Thus for an observer in an external region we have the following situation: the domain of dependence of the initial region exterior to the horizon is the same as that of a single BTZ black hole. However, prior to the past Cauchy horizon the geometry is different from that of a single black hole. The observer in one exterior region can see events from the the other black hole region, for example the other “white hole” singularity. By looking at the past, an external observer can tell that she is in a multi-black-hole spacetime, although no experiments she can do in the future will reveal this.

## V. Black Holes with Angular Momentum

The general BTZ black hole has angular momentum. It therefore has no global totally geodesic spacelike surfaces to simplify an initial value description. We therefore treat it from the spacetime point of view. Because adS space is the universal cover, black holes with angular momentum can still be considered a piece of adS space, suitably identified. In fact, one can use the same piece, and the same identification surfaces, as those shown in Figures 9 and 10. The only difference is that the isometry that defines the identification is not simply a “boost” about a geodesic (which would become the non-Hausdorff singularity), but in addition it involves a boost within an identification surface. For example, in Figure 9 it could be a boost in the Minkowski disk of the figure’s left half, with fixed point at the origin — that is, a displacement of the BTZ time-coordinate in that plane. This boost leaves the geodesic labeled  $r = 0$  invariant, but moves the points within that geodesic, so that the geodesic is no longer a set of fixed points, and hence no singularity occurs there. (With this “boosted” identification, this geodesic also no longer has BTZ coordinate  $r = 0$ , because  $r$  measures the circumference of the circle at constant  $r$ , and that is now the finite amount by which points move on that geodesic.)

Although the boosted identification has no fixed points, there is still a line with  $r_{BTZ} = 0$ , namely the one that connects identified points and that is *lightlike*. (This would occur somewhere in the region that is spacelike related to the geodesic labeled  $r = 0$  in Fig. 9). Beyond that line, timelike curves connect identified points. Therefore the line  $r_{BTZ} = 0$  is still considered a kind of singularity, since it bounds a region of closed timelike curves.

Can we make a similar boosted identification in the multi-black-hole case? The condition is that the spacetime should look like a single BTZ black hole with angular momentum in each asymptotic region. A possible problem is that a boost about one horizon line is a timelike motion at the neighboring horizon lines, but there should be no net timelike motion as one goes once around all the black holes and comes back to the starting point — else we would get closed timelike lines everywhere. Therefore not all the angular momenta can be chosen arbitrarily. It can however be shown [2] that, with a sufficient number of black holes, multi-black-hole configurations with angular momenta are possible.

## VI. Analogous 3+1 Dimensional Black Holes

The BTZ black holes can be generalized in various ways to 3+1 dimensional gravity with negative cosmological constant. Thus one can obtain black hole configurations of various topologies and horizon structures. For example, the following metrics are solutions of Einstein’s equations [7]:

$$ds^2 = -F dt^2 + \frac{dr^2}{F} + r^2(d\theta^2 + \theta^2 d\phi^2) \quad \text{with} \quad F = -\frac{2m}{r} + \frac{r^2}{\ell^2} \quad (8)$$

$$ds^2 = -F dt^2 + \frac{dr^2}{F} + r^2(d\theta^2 + \sinh^2 \theta d\phi^2) \quad \text{with} \quad F = -1 - \frac{2m}{r} + \frac{r^2}{\ell^2}. \quad (9)$$

In a sense these interpolate between BTZ-type metrics of constant curvature, and Schwarzschild-type metrics, with curvature increasing with decreasing  $r$ . If we annul the Schwarzschild mass parameter  $m$  we obtain metrics for 3+1 adS space written in BTZ-type coordinates. The first metric is an analog of a BTZ metric with  $M = 0$ , and the second metric is analogous to one with  $M = 1$ . (These can be obtained from the well-known Schwarzschild-deSitter metric by the substitution  $\Lambda = 1/\ell^2$ ,  $\theta \rightarrow i\theta$ ,  $r \rightarrow ir$ ,  $t \rightarrow it$ ,  $m \rightarrow im$ .)

In order that these metrics describe black holes even when  $m = 0$  we need again to make identifications. In Eq (8) the surfaces  $r = \text{const}$ ,  $t = \text{const}$  are flat, with  $\theta$ ,  $\phi$  acting as polar

coordinates. Such flat surfaces (with constant extrinsic curvature) are known in the Poincaré ball as *horospheres* — they are spheres that touch the limit sphere at one point, the point at infinity of the flat surface. We can change these to finite surfaces by means of a torus identification; that is, we identify  $x = \theta \cos \phi$  and  $y = \theta \sin \phi$  periodically. The result is an “extremal” BTZ-type black hole, with an infinitely long, toroidal throat.

For a black hole with a finite throat we use the metric of Eq (9) and note that the surfaces  $r = \text{const}$ ,  $t = \text{const}$  have negative intrinsic curvature. As we found out above (for example, fig. 6), by identifications such spaces can be given finite area (and topology with negative Euler characteristic). This area has a finite minimum on the initial surface at the horizon, where  $F = 0$ .

The horizons of these black holes have various, non-spherical topologies. This does not violate any horizon theorems, because infinity ( $\mathcal{I}$ ) has the same unusual topology. For further examples of non-standard, asymptotically anti-de Sitter, black holes see [8]. Multi-black-hole geometries can similarly be constructed [7].

## VII. Conclusions

We have seen a remarkable variety of black hole configurations that are possible in spaces of negative cosmological constant, even when the gravitational field does not have local degrees of freedom. The exteriors of such configurations have a timelike Killing vector and are therefore static or stationary. The interior has nontrivial time development, which can largely be derived from the Raychaudhuri equation. Because even complicated examples can be constructed rather explicitly it is likely that these solutions will be useful testing grounds for new ideas about black hole physics.

## References

- [1] M. Bañados, C. Teitelboim, and J. Zanelli, Phys. Rev. Lett. **69**, 1849 (1992)
- [2] D. Brill, Phys. Rev. D**53**, R4133 (1996)
- [3] A. Steif, Phys. Rev. D**53**, 5527 (1996)
- [4] S. Deser, R. Jackiw, and G. t’Hooft, Ann. Phys. **152**, 220 (1984)
- [5] C. W. Misner, Phys. Rev. **118**, 1110 (1960)
- [6] Bengtsson, Brill, et al (to be published)
- [7] Brill and Louko (to be published)
- [8] Áminneborg, Bengtsson, Holst and Peldán, *Making Anti-de Sitter Black Holes*, gr-qc/9604005.

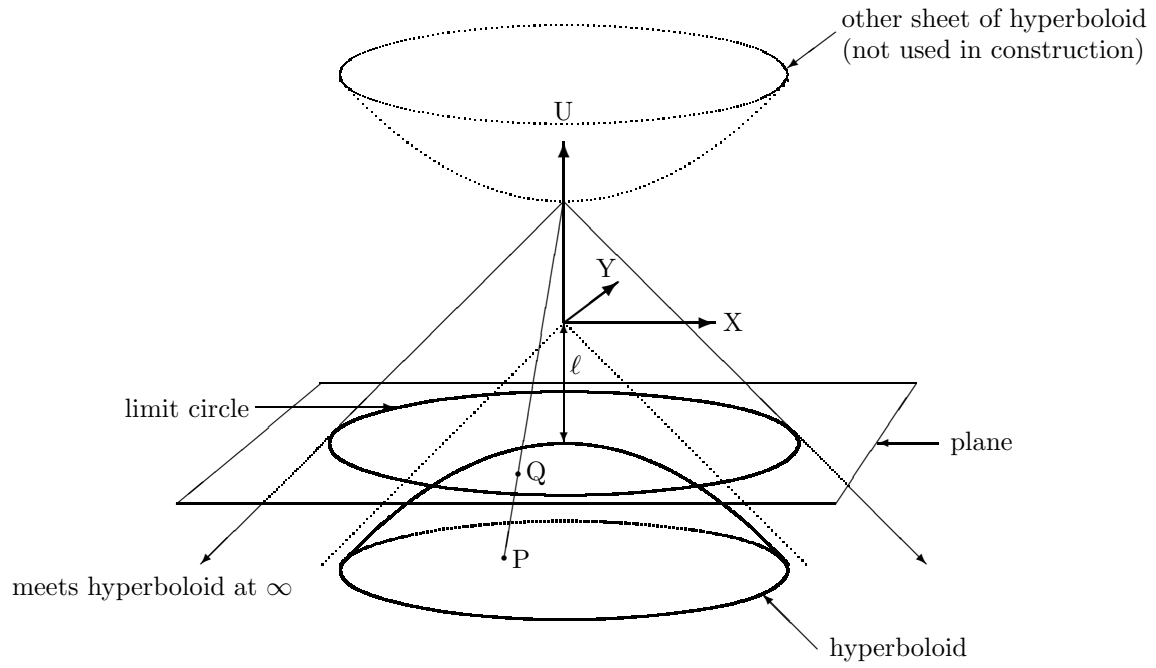


Figure 1: Stereographic projection of a spacelike hyperboloid of constant curvature in Minkowski space on a plane. Point  $P$  in the hyperboloid projects to point  $Q$  in the plane. The hyperboloid is the intersection of 2+1 adS space, Eq (2), with the plane  $T = 0$ .

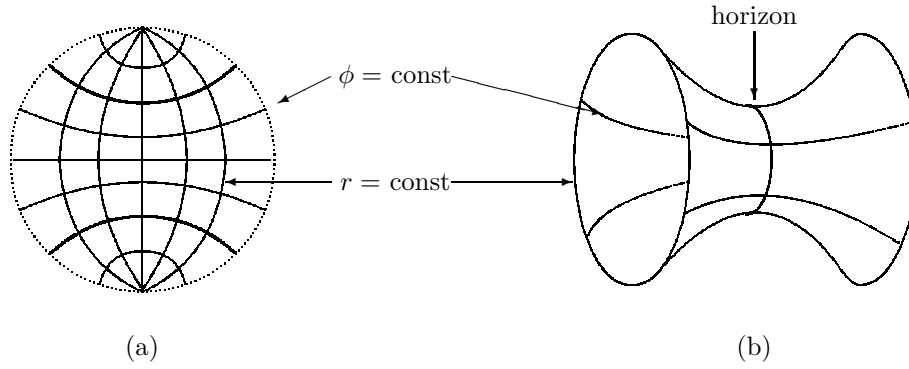


Figure 2: a. BTZ coordinate lines  $r, \phi$  on the Poincaré disk, centered at the horizon. All coordinate lines have constant curvature and therefore appear as (parts of) circles. The lines  $\phi = \text{const}$  have zero curvature (geodesics) and are mutually ultraparallel. In the BTZ black hole the lines  $\phi = 0$  and  $\phi = 2\pi$  (drawn thick) are identified. b. Sketch of part of the surface obtained by identification. The asymptotic region at large  $r$  cannot be embedded into flat space.

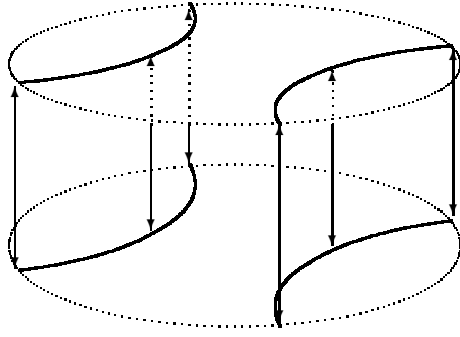


Figure 3: Constructing the initial state of a BTZ black hole by doubling a strip of the Poincaré disk bounded by two ultraparallel geodesics.

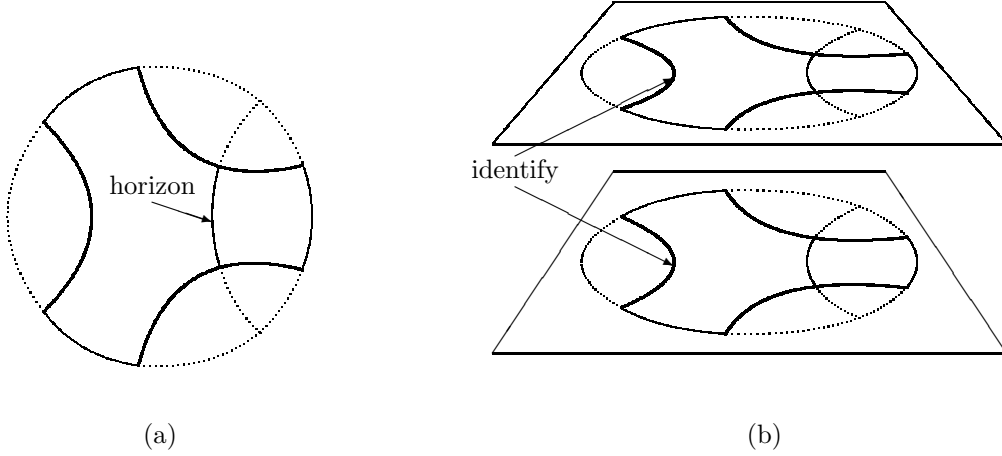


Figure 4: Construction of a three-black-hole initial geometry by doubling a region bounded by three geodesics in the Poincaré disk.

(a) Half of the initial geometry is represented by the region bounded by the thick circular arcs. The horizon of one black hole region (minimal geodesic between the two geodesics on the right) is shown. The other two horizons can be obtained by  $120^\circ$  rotations.

(b) Two disks are placed one above the other, and the thick boundaries are identified vertically, as shown explicitly for the boundary on the left.

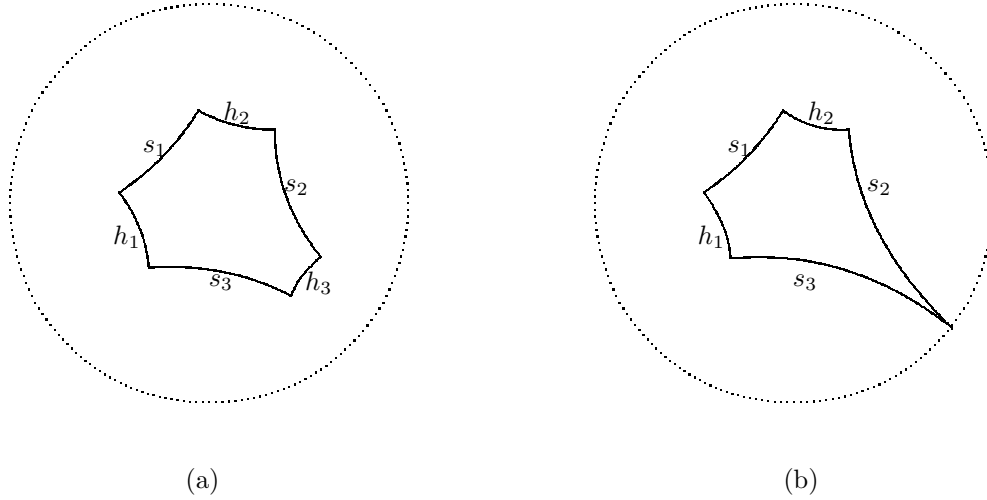
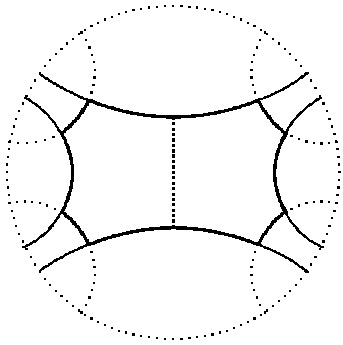


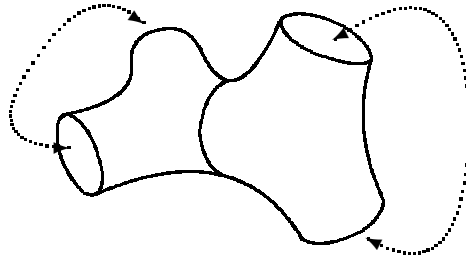
Figure 5: The parameters of multi-black-hole initial states obtained by doubling a right-angle polygon with an even number of sides.

(a) A hexagon represents three horizons  $h_i$  and three distances  $s_i$ .

(b) In the limit  $h_3 \rightarrow 0$  (hence  $M_3 \rightarrow 0$ ) the hexagon degenerates into a pentagon with one corner at infinity.



(a)



(b)

Figure 6: (a) A diagram for four black holes can be thought of as two three-black-hole configurations joined at the thick dotted line.

(b) A 3D picture to give an idea of the result of cutting the four-black-hole configuration at the thick dotted line, rotating, and rejoining.



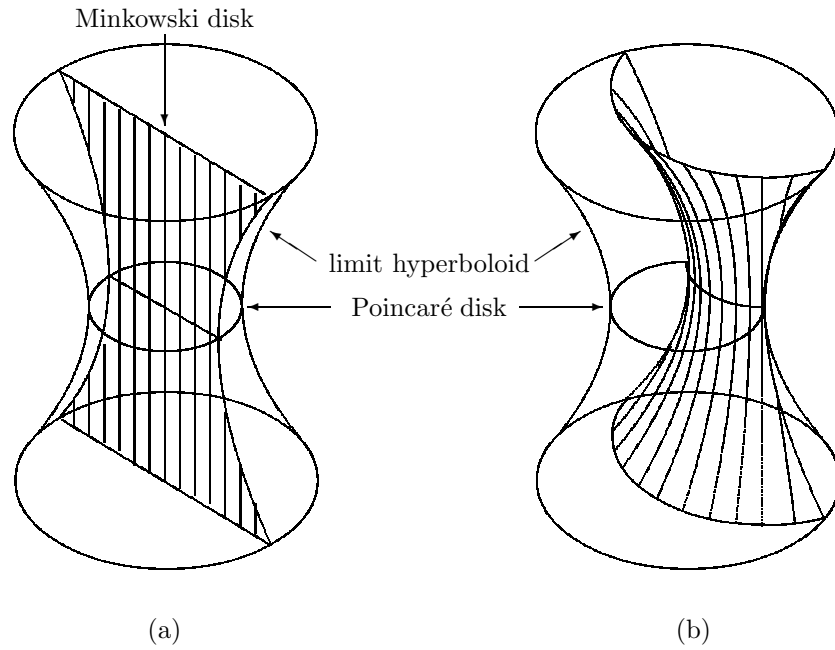


Figure 8: The Minkowski ball and two totally geodesic surfaces in it, both normal to the same Poincaré disk. The totally geodesic subspaces are striped only for identification, the lines (except the central one) are not geodesics.

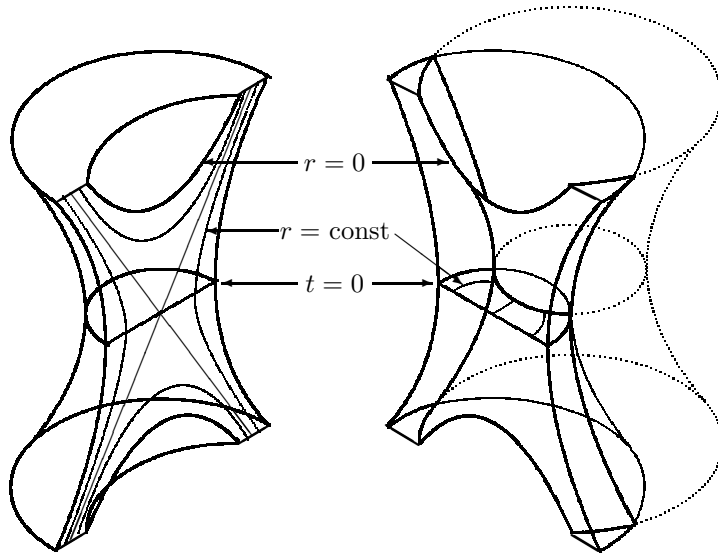


Figure 9: The two Minkowski disks of Fig. 8 in a single picture. To show more clearly the one that is part of a hyperboloid, the rest of that hyperboloid is drawn dotted.

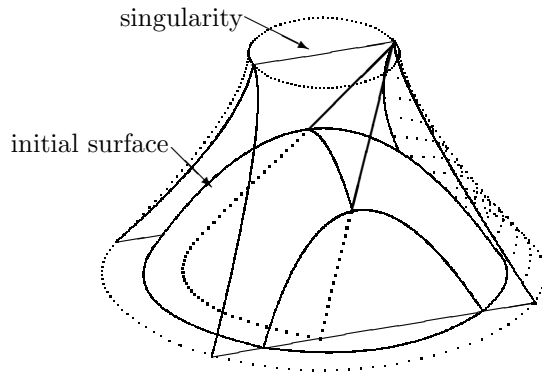


Figure 10: Stereographic projection of a BTZ black hole centered on the non-Hausdorff singularity. The two planes that intersect in the singularity are to be identified. One of the regions  $\mathcal{F}$  is shaded with dots, and its horizon is shown in heavy outline. (The initial surface is drawn as non-transparent, except for the horizon. Therefore we do not see the hyperbolic intersection of the plane in the back with the initial surface.)

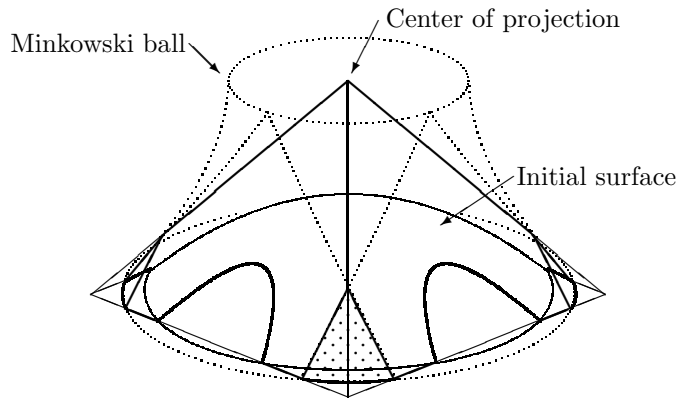
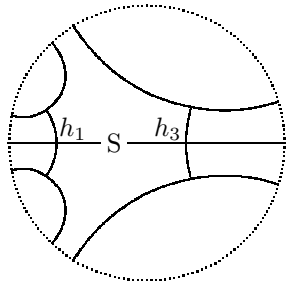


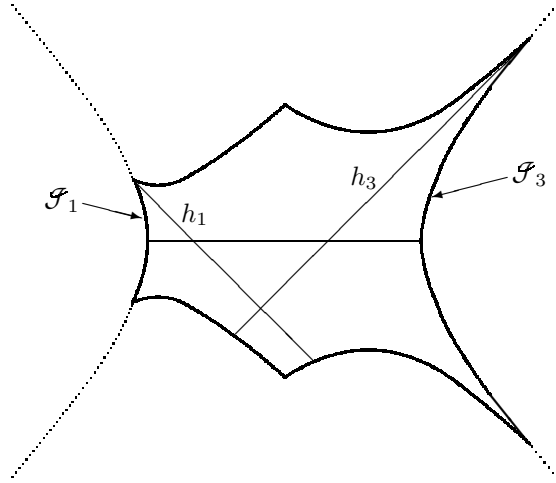
Figure 11: A four-black-hole spacetime in stereoscopic projection centered on the singularity. As before the physical region should be doubled, with identifications along the sides of the pyramid. Other identifications are also possible.<sup>7</sup> One of the four  $\mathcal{S}$ 's is shaded by dots.

---

<sup>7</sup>I am indebted to the group of Bengtsson at Stockholm, particularly to Sören Holst, for clarifying several features of this figure. Also see [6].



(a)



(b)

Figure 12: (a) A four-black-hole initial geometry and a line of symmetry,  $S$ .  
 (b) The spacetime development of the line of symmetry.